Available online at www.sciencedirect.com

SciVerse ScienceDirect

Procedia CIRP 8 (2013) 152 – 157

www.elsevier.com/locate/procedia

14th CIRP Conference on Modeling of Machining Operations (CIRP CMMO)

On the SPH Orthogonal Cutting Simulation of A2024-T351 Alloy

Martin Madaj[a,]*, Miroslav Píška[a]

[a]Brno University of Technology, Institute of Manufacturing Technology, Technická 2896/2, Brno 61669, The Czech Republic

* Corresponding author. Tel.: +420-541-142-420; fax: +420-541-142-555. *E-mail address*: madaj@fme.vutbr.cz.

Abstract

Smoothed Particle Hydrodynamics (SPH) is known for its ability to simulate a natural flow of material without mesh distortion problems related to the Finite Element Method (FEM) frequently. Therefore it can be used to simulate material flow around the tooltip in machining simulations.

This paper presents some results of the SPH orthogonal cutting simulations of A2024-T351 aluminium alloy compared to the experimental and FEM simulation results published by Mabrouki et al. recently. Simulations were performed with the ANSYS LS-DYNA solver. To simulate the workpiece behavior during cutting, the Johnson-Cook constitutive material model was used. In this work, an influence of the Johnson-Cook failure parameters D1-D5 and SPH density on a saw-toothed chip formation was observed. Chip shapes, von Mises stress, plastic strains, strain rates and cutting forces were compared to published results, confirming that the SPH method is able to predict the cutting and feed forces and the chip shape correctly. For experimental verification, a CNC machine, dry cutting, uncoated cemented carbide inserts ISO N10-20, cutting speeds in the range of 200-800 m/min, feed 0.4 mm and depth of cut 4.0 mm were used. Regarding the SPH particles density it was found that the model with smaller space among particles tended to form a highly segmented chip. However, for a good correlation with experimental results the Johnson-Cook failure parameters together with minimum required strain for failure should be set.

Selection and peer-review under responsibility of The International Scientific Committee of the "14th CIRP Conference on Modeling of Machining Operations" in the person of the Conference Chair Prof. Luca Settineri

Keywords: Cutting; FEM; Chip; Modelling; SPH

1. Introduction

Cutting simulations are widely used to study and predict behaviour of various materials under different cutting conditions with combinations of different tool geometries. Many of these simulations can be used to simulate behaviour of a brand new, still not physically produced cutting tool. 2D (orthogonal) and 3D (oblique) simulations are performed using various numerical methods. Finite Element Method (FEM) is the most common method to simulate cutting. Depending on its type (Lagrangian, Eulerian, Arbtitrary Lagrangian-Eulerian) it may suffer from excessive mesh distortion (leading to a negative element volume) that may cause the simulation to stop. To overcome this issue, an adaptive remeshing may be used [1].

On the contrary, Smoothed Particle Hydrodynamics (SPH) method is one of the meshless particle methods that can handle very large deformations occurring during cutting without limitations related to FEM [1] and with no need of remeshing. This attribute of the SPH method can be considered as the most important and advantageous compared to FEM. If the metal cutting should be simulated using the FEM method, it is necessary to set up parameters allowing the material failure and separation caused by the cutting tool. This can be done via adaptive remeshing and/or element deletion. Adaptive remeshing can be time consuming, whereas the element deletion leads to removing of the mass from the calculation – therefore the element size should be sufficiently small to minimize the effect of the element deletion. Using the SPH method, none of the above mentioned techniques is necessary – material separation is implemented directly in the SPH method through a loss of cohesion among particles and therefore the calculation is not influenced by the loss of the workpiece mass [2].

Selection and peer-review under responsibility of The International Scientific Committee of the "14th CIRP Conference on Modeling of Machining Operations" in the person of the Conference Chair Prof. Luca Settineri

doi:10.1016/j.procir.2013.06.081

Although some authors used the SPH to simulate the cutting process, it can be seen (i.e. by reviewing the content of some scientific databases) that it is not as commonly used as FEM method.

The SPH method is described in detail in the book by G. R. Liu and M. B. Liu [1] or e.g. in the article by Monaghan [3]. Practical aspects of the SPH method related primarily to cutting simulations were discussed particularly by Limido et al. [4], Villumsen and Fauerholdt [5], Espinosa et al. [6] or Schwer [7].

Villumsen and Fauerholdt [5] performed a 3D orthogonal cutting simulation of Al 6082-T6 alloy and described some important LS-DYNA contact settings, boundary conditions, material properties and EOS (Equation of State) settings. Subsequently they performed sensitivity analysis to evaluate an influence of a particle pitch, mass scaling, the cutting speed and a friction coefficient on the cutting and thrust forces.

Espinosa et al. [6] compared the SPH and classical simulation approaches and discussed other important simulation settings, specifically an artificial viscosity and a renormalized SPH formulation. Regarding the artificial viscosity, they proposed to change a linear component (Q2) value from default 0.06 to 0.50. This change significantly enhanced a "smoothness" of von Mises stress. Renormalized SPH formulation is useful especially in cutting simulations because it helps to form the chip shape in a better way than a classical formulation. Using the classical approximation the chip shape is too straight whereas the renormalized SPH formulation leads to more realistic (curved) chip.

Schwer's paper [7] is related to the SPH simulations of aluminium plate perforation but he stated some important notes on the artificial bulk viscosity and the Johnson-Cook failure model. At first, he was informed by Lacome (developer of SPH in LS-DYNA) that the linear viscosity coefficient Q2 should be increased from default 0.06 to 1.00 – this corresponds to Espinosa et al. [6] who proposed increasing of Q2 to 0.5. Increased value of the linear viscosity caused residual particles speeds to fall to some unexpectedly low values. Due to that change Schwer proposed to include the Johnson-Cook failure parameters into the SPH simulation. Since the SPH method itself allows a material separation (i.e. [5], [8]), Johnson-Cook failure parameters normally need not to be defined. As a result, residual particle speeds changed to values more realistic to the observed residual speeds. This finding has proved itself to be useful also in this paper.

The aim of this paper is to compare the SPH orthogonal cutting simulation of A2024-T351 alloy to the FEM simulation and experimental results performed by Mabrouki et al. [9] and to prepare the basic simulation settings for future extension to drilling and milling simulations. Simulations were performed with ANSYS LS-DYNA solver.

2. Experiment and SPH model settings

All experimental and simulation parameters were chosen accordingly to Mabrouki's et al. paper and thus all the results could be easily compared and evaluated.

2.1. Settings of the experiment

A2024-T351 aluminium alloy was selected to be cut by the uncoated carbide insert CCGX120408-AL, H10, (Sandvik Coromant) with the orthogonal rake angle γ_o = 17.5° and a tip radius of 20 µm. The cutting speed v_c was set to 200 m/min and 800 m/min, the depth of cut was constant (a_p = 4 mm) and the feed per revolution was set to f = 0.4 mm. The cutting force was measured by the Kistler dynamometer 9257B with the Kistler charge amplifier 5070.

2.2. SPH analysis settings

The SPH model (see Fig. 1) consisted of a rigid tool (FEM elements) and an SPH workpiece. The tool was constrained in y and z direction with imposed motion in x direction. The workpiece dimensions were 5.8 x 1.0 x 0.05 mm and it consisted of 18560 SPH particles – therefore the SPH particle spacing was 0.025 mm. To constrain the workpiece, all translational degrees of freedom were removed on its left and bottom SPH nodes.

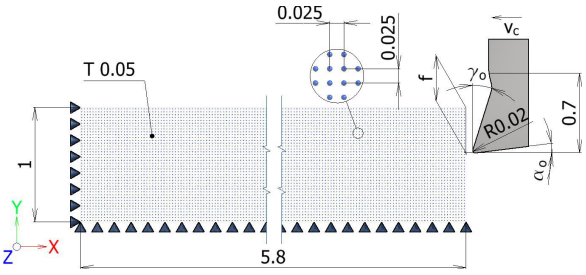

Fig. 1. SPH model scheme

Regarding the SPH model nominal width in z direction (0.05 mm), it is necessary to multiply the predicted force values by the factor of 80 to get the force values corresponding to the experimentally obtained values (depth of cut/width = 4/0.05 = 80).

2.2.1. Tool and workpiece physical properties and material model

Physical properties of the workpiece and the tool are listed in Table 1. Johnson-Cook material model and failure parameters can be found in Table 2.

Table 1. Workpiece and tool physical parameters [9]

Physical property	Workpiece	Tool
Density ρ [kg/m^3]	2700	11900
Elastic modulus E [GPa]	73	534
Poisson's ratio μ [-]	0.33	0.22
Specific heat Cp [J/kgK^{-1}]	875	-
T_{melt} [K]	1793	-
T_{room} [K]	300	300

Table 2. Johnson-Cook parameters of A2024-T351 material [9]

Parameter	A [MPa]	B [MPa]	n [-]	C [-]	m [-]
Value	352	440	0.42	0.09	1.03
Parameter	D1 [-]	D2 [-]	D3 [-]	D4 [-]	D5 [-]
Value	0.13	0.13	-1.5	0.011	0

2.2.2. Friction coefficient

According to [9] and [10] Coulomb friction model was used with static (μ_s) and dynamic (μ_d) friction coefficients set to 0.17 [11]. If the contact was SPH/SPH only, the friction coefficient need not to be defined [6] but an influence of the friction coefficient on pure SPH/SPH simulation was not further investigated. The model presented here includes the SPH/FEM contact.

3. Results and discussion

The following section presents particularly the SPH simulation results. Predicted cutting force values, chip shapes, plastic strain and strain rates are presented and compared to Mabrouki's FEM simulation. Also other investigations, i.e. the influence of the Johnson-Cook failure parameters, are presented and discussed.

3.1. Results of the experiment

The cutting force average values are listed in Table 3. Fig. 2 shows an example of the chip shape for the cutting speed v_c = 200 m/min.

Fig. 2. Example of the chip shape for the cutting speed v_c = 200 m/min

3.2. SPH simulation results

3.2.1. Cutting force values

Predicted cutting force values for v_c = 200 m/min are presented in Fig. 3, values for v_c = 800 m/min are presented in Fig. 4. Values for v_c = 400 m/min are presented only in Table 3.

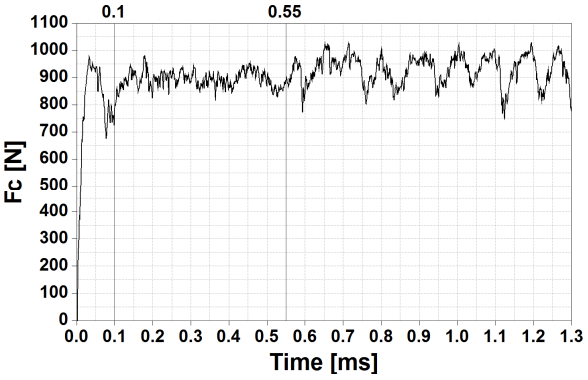

Fig. 3. Cutting force, v_c = 200 m/min

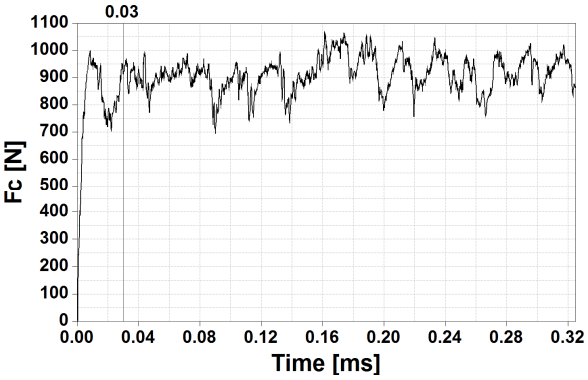

Fig. 4. Cutting force, v_c = 800 m/min

A comparison of experimentally obtained and simulated force values is in Table 3. Average simulated force values were computed from the time of 0.10 ms (200 m/min), 0.065 ms (400 m/min) and 0.03 ms (800 m/min) respectively. A graphical summary of the cutting force evolution caused by different cutting speeds together with experimental and FEM results is shown in Fig. 5.

The comparison of the experimental and the simulated forces data (Table 3 and Fig. 5) showed that SPH method is able to predict the cutting force values very close to the experimental values and to the values obtained using the finite element method (although, for this test case, there's a relatively high difference in cutting force values between SPH and FEM [9] for v_c = 400 m/min compared to v_c = 200 m/min and 800 m/min). Generally speaking, apart from the FEM [9] average cutting force value for v_c = 400 m/min, the

evolution of cutting force values predicted by SPH is similar to the experimentally obtained results, even though the force values are slightly underestimated.

Table 3. Comparison of average cutting force values

Cutting speed [m/min]	200	400	800
Force [N]	F_c	F_c	F_c
Experiment	996.12	990.30	987.01
Experiment [12]	988	978	976
SPH simulation	916.16	905.52	915.31
FEM simulation [9]	898	994	901
Comparison	Difference [%]		
SPH vs. experiment	-8.03	-9.36	-7.26
SPH vs. experiment [12]	-7.84	-8.00	-6.22
SPH vs. FEM [9]	1.98	-9,77	1.59

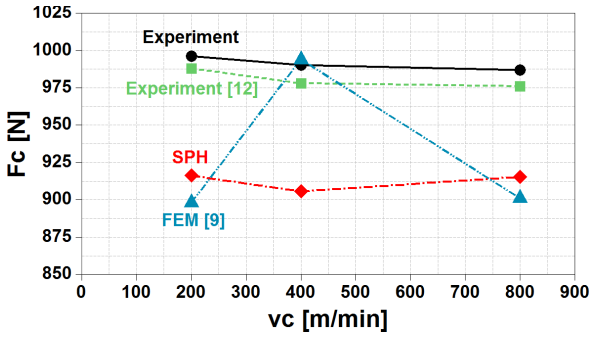

Fig. 5. The cutting force evolution with different cutting speeds

In order to save some computational time in future SPH simulations, Villumsen and Fauerholdt [5] performed a sensitivity analysis to evaluate possible influence of the cutting speed on the cutting forces. Their results showed that every increase in the cutting speed leads to the increase in cutting force values. Results presented in this paper do not correspond well with results presented in [5] (see SPH line in Fig. 5 or values in Table 3) – cutting force values do not increase significantly with increasing of the cutting speed. Such a discrepancy may be due to the different Johnson-Cook material model parameters or due to the different SPH method settings (especially the influence of Johnson-Cook failure parameters and the presence of a tooth-shaped chip should be considered).

The cutting force values for v_c = 200 m/min (see Fig. 3) at the time interval 0.10-0.55 ms are less fluctuating compared to values above 0.55 ms time limit. This corresponds to the continuous chip formation without segmentation. Segmentation occurs from the time 0.55 ms and later when the chip touches the workpiece surface and thus the chip bending moment occurs. Chip segmentation is accompanied with increasing plastic strain values in the primary shear zone, see Fig. 6 (b) and (c).

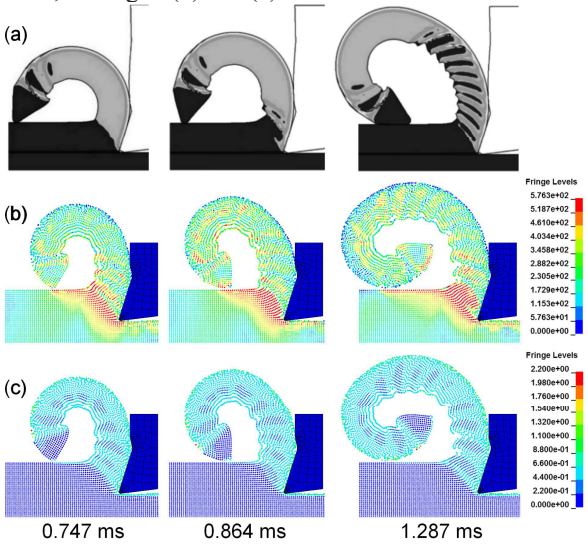

Fig. 6. (a) reference chip shape according to [9], (b) chip shape and von Mises stress distribution for SPH simulation, (c) plastic strain distribution for SPH simulation; v_c = 200 m/min

On the contrary, when cutting with v_c = 800 m/min, no continuous chip is obtained (Fig. 7), no less fluctuating region is observed at the cutting force values (Fig. 4) and the simulated chip is tooth-shaped.

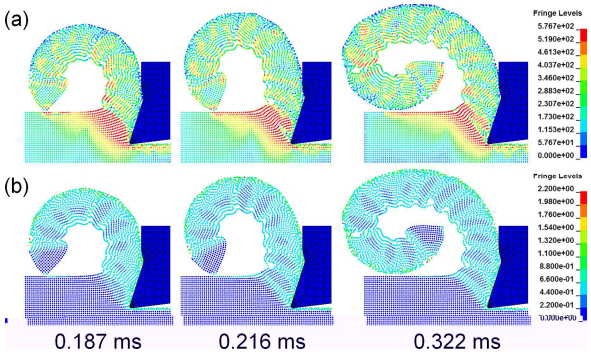

Fig. 7. (a) chip shape and von Mises stress distribution for SPH simulation, (b) plastic strain distribution for SPH simulation; v_c = 800 m/min

3.2.2. Chip shape, von Mises stress, and plastic strain

Fig. 6 (a) shows the reference FEM chip shape [9], the chip shape obtained by the SPH method (Fig. 6 (b) and (c)), the von Mises stress (Fig. 6 (b)) and plastic strain (Fig. 6 (c)). Values and chip shapes are displayed for the cutting speed of 200 m/min at three time points: 0.747 ms, 0.864 ms and 1.287 ms.

The chip shape and the distribution of von Mises stress with plastic strain for v_c = 800 m/min is shown in Fig. 7 (a) and (b). Maximum value of von Mises stress in

chip is about 576 MPa, Mabrouki [9] gives values about 600 MPa. Chip shape is presented at three time points (0.187 ms, 0.216 ms and 0.322 ms) to show the difference between segmentation in chip (compare with Fig. 6) while the tool machined the same distance on the workpiece as for the cutting speed of 200 m/min.

3.2.3. Deformation speed

Influence of the cutting speed on the deformation speed $\dot{\varepsilon}_{pl}$ can be seen in Fig. 8. Deformation speeds are displayed only for five reference elements selected in the middle of the workpiece. Cutting speed v_c = 800 m/min caused significantly higher deformations speeds than cutting speed v_c = 200 m/min – i.e. for the element 9496 the maximal deformation speed is about 134 s^{-1} which is approximately 8.93 times higher than 15 s^{-1} for v_c = 200 m/min

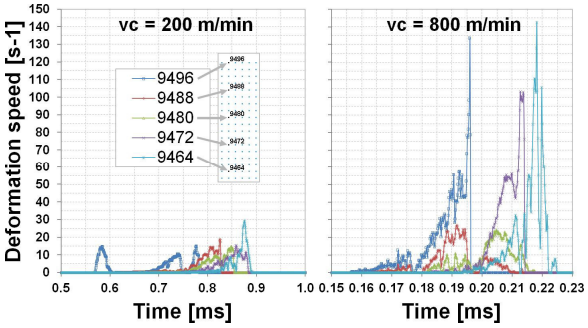

Fig. 8. Deformation speeds for selected SPH elements

3.2.4. Influence of the friction coefficient

Since the both of FEM elements and SPH particles were used to model the tool/chip interface, the friction coefficient has to be set. To evaluate possible influence of the friction coefficient on the cutting force values, three different values of static (μ_s) and dynamic (μ_d) friction coefficient were used in simulations with cutting speed of 800 m/min. The values used were 0, 0.17 (default value from [11]) and 0.34.

Changes to the static and dynamic friction coefficient influenced the chip shape, plastic strain values and cutting force values. Influence on the chip shape is presented in Fig. 9. The higher is the friction coefficient, the higher is the chip radius, and accordingly the lower is the chip curvature. Also a shear plane angle as well as the chip thickness was influenced – higher friction coefficient values caused the shear plane angle was lower and the chip was thicker and vice versa. Plastic strain values were higher when the higher value of friction coefficient was used. It is worth noting that setting the single-surface contact to treat the workpiece (chip) self-contact with the friction coefficient value had no effect on the simulation.

Influence of the friction coefficient on the cutting forces can be seen in Fig. 10. The cutting forces were friction coefficient-dependent, higher average cutting force values were obtained with higher friction values.

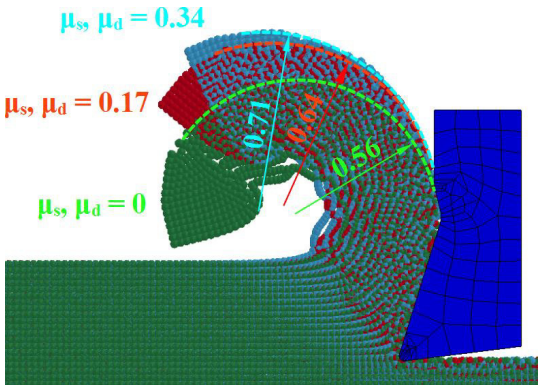

Fig. 9. Chip shapes influenced by the friction coefficient values; v_c = 800 m/min, 0.1131 ms

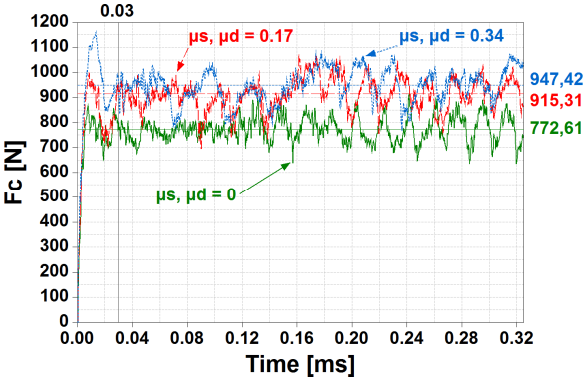

Fig. 10. The cutting force evolution in time for different friction coefficient values; v_c = 800 m/min

3.2.5. Influence of the Johnson-Cook failure parameters on the chip shape

According to [5] or [8] suggestion, first attempts to run the SPH orthogonal cutting simulation of A2024-T351 alloy have been made without setting the Johnson-Cook failure parameters (D1-D5 values were equal to 0). Also the EFMIN value (the minimum required strain for failure or the lower bound for strain at fracture [13]) was set to its default (0.000001) value. This led to a continuous chip creation without any evidence of the segmentation even at the cutting speed of 800 m/min. Example of the chip with plastic strain distribution at the time step 0.322 ms can be seen in Fig. 11.

According to [7] the Johnson-Cook failure parameters were involved but EFMIN was still set to the default value. The both of previously mentioned settings caused the high chip segmentation even at cutting speed of 200 m/min (see Fig. 12 at the timestep 1.287 ms). No steady state chip formation region (as can be seen in

Fig. 6 (b) and (c) and the cutting force chart in Figure 3) was observed.

As a next step, the EFMIN value was set for both simulations to reduce the chip segmentation. Usable EFMIN value was determined by a trial and error method and was of 0.65 for both of the simulations.

However, involving the EFMIN value might not be quite adequate because it artificially restricts the amount of the plastic strain in the chip before the fracture occurs.

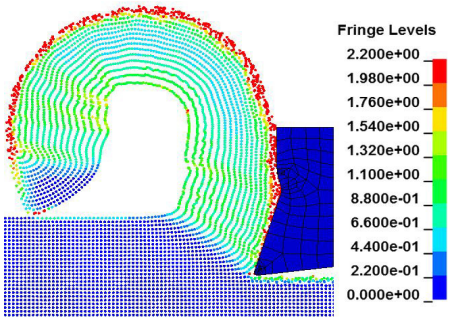

Fig. 11. Chip shape and plastic strain distribution; v_c = 800 m/min

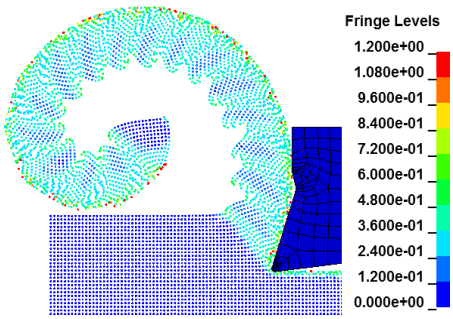

Fig. 12. Chip shape and plastic strain distribution; v_c = 200 m/min

3.2.6. Influence of the SPH particles density

When testing the different model settings, some results indicated that the chip shape might also be influenced by the SPH particle spacing and by the SPH smoothing length related parameters CSLH, HMIN and HMAX. For example, different chip shapes (from continuous to discontinuous) were observed for cutting speed of 800 m/min when the particle spacing was set to 0.00625 mm (thousandths of mm in general) with various settings of smoothing length parameters. Johnson-Cook failure parameters (including EFMIN) were omitted. But the above hypothesis needs to be further investigated because no obvious correlation among the particle spacing, the smoothing length parameters and the chip shape was found.

4. Conclusions

Findings presented in this paper indicate that the SPH method is able to predict the chip shape and the cutting force in a good correlation with experiment and finite element simulation (for orthogonal cutting simulation). However, to observe the chip segmentation, it might be necessary to use the Johnson-Cook failure parameters and the minimum required strain for failure value. Also it must be noted that different material model parameters and other material models themselves should be further tested to examine their usability for SPH cutting simulations.

Acknowledgements

This research work was supported by the BUT, Faculty of Mechanical Engineering, Brno, Specific research 2011, with the grant "Research of advanced CNC methods for perspective applications", FSI-S-11-28, ID 1438.

References

[1] Liu, G. R., Liu, M. B., 2003, Smoothed Particle Hydrodynamics – A Meshfree Particle Method, World Scientific Publishing Co. Pte. Ltd., Singapore.

[2] Heinstein, M., Segalman, D., 1997, Simulation of Orthogonal Cutting with Smooth Particle Hydrodynamics, Sandia report SAND97-1961, Sandia National Laboratories, Albuquerque, New Mexico and Livermore, California.

[3] Monaghan, J. J., 2005, Smoothed particle hydrodynamics, Rep. Prog. Phys., 68:1703-1759.

[4] Limido, J., Espinosa, C., Salaün, M., Lacome, J. L., 2007, SPH method applied to high speed cutting modeling, International Journal of Mechanical Sciences, 49/7:898-908.

[5] Villumsen, M. F., Fauerholdt, T. G., 2008, Simulation of Metal Cutting using Smoothed Particle Hydrodynamics, 7. LS-DYNA Anwenderforum, C-III-17–C-III-36.

[6] Espinosa, C., Lacome, J. L., Limodo, J., Salaün, M., Mabru, C., Chieragatti, R., 2008, Modelling High Speed Machining with the SPH Method, 10th International LS-DYNA Users Conference, 12-9–12-20.

[7] Schwer, L. E., 2009, Aluminium Plate Perforation: A Comparative Case Study Using Lagrange with Erosion, Multi-Material ALE, and Smooth Particle Hydrodynamics, 7th European LS-DYNA Conference.

[8] Gallet, C., Lacome, J. L., 2002, S.P.H.: A Solution to Avoid Using Erosion Criterion? DYNAlook.

[9] Mabrouki, T., Girardin, F., Asad, M., 2008, Numerical and experimental study of dry cutting for an aeronautic aluminium alloy (A2024-T351), International Journal of Machine Tools and Manufacture, 48/11: 1187-1197.

[10] Hallquist, J. O., 2006, LS-DYNA Theory Manual, Livermore Software Technology Corporation, California.

[11] Asad, M., 2010, Elaboration of Concepts and Methodologies to Study Peripheral Down-cut Milling Process from Macro-to-Micro Scales, Institut National des Sciences Appliques de Lyon.

[12] Asad, M., Girardin, F., Mabrouki, T., Rigal, J.-F., 2008, Dry cutting study of an aluminium alloy (A2024-T351): a numerical and experimental approach, 11th ESAFORM2008 conference on material forming, Lyon, France.

[13] Livermore Software Technology Corporation (LSTC), 2012, LS-DYNA: Keyword User's Manual – Volume II: Material Models, California.